ISSN: 0976 – 9102 (ONLINE)
DOI: 10.21917/ijivp.2010.0010

FAST DISCRETE CURVELET TRANSFORM BASED ANISOTROPIC FEATURE EXTRACTION FOR IRIS RECOGNITION

Amol D. Rahulkar[1], Dattatraya V. Jadhav[2] and Raghunath S. Holambe[3]

[1]*Department of Instrumentation and Control Engineering, AISSMS Institute of Information Technology, Maharashtra, India*
E-mail: amolrahulkar_000@yahoo.com

[2]*Department of Electronics and Telecommunication Engineering, Bhivarabai Sawant College of Engineering and Research, Maharashtra, India*
E-mail: dvjadhao@yahoo.com

[3]*Department of Instrumentation Engineering, SGGS Institute of Engineering and Technology, Maharashtra, India*
E-mail: holambe@yahoo.com

Abstract

The feature extraction plays a very important role in iris recognition. Recent researches on multiscale analysis provide good opportunity to extract more accurate information for iris recognition. In this work, a new directional iris texture features based on 2-D Fast Discrete Curvelet Transform (FDCT) is proposed. The proposed approach divides the normalized iris image into six sub-images and the curvelet transform is applied independently on each sub-image. The anisotropic feature vector for each sub-image is derived using the directional energies of the curvelet coefficients. These six feature vectors are combined to create the resultant feature vector. During recognition, the nearest neighbor classifier based on Euclidean distance has been used for authentication. The effectiveness of the proposed approach has been tested on two different databases namely UBIRIS and MMU1. Experimental results show the superiority of the proposed approach.

Keywords:
Iris Recognition, Biometrics, Curvelet Transform, FDCT, Feature Extraction

1. INTRODUCTION

Establishing the identity of a person is becoming critical in our vastly interconnected society. The need for reliable person authentication techniques has increased in the wake of high concerns about security and rapid advancement. Biometrics is described as the science of recognizing an individual based on physiological or behavioral traits. Biometrics has become popular over the traditional token based or knowledge based techniques (e.g. identification card, passwords, PIN, etc.). This is because of the ability of biometrics technology to differentiate between an authorized person and an imposter efficiently.

Iris based recognition is the most promising for high security environment among various biometric techniques (face, fingerprint, palm vein, signature, palm print, etc.). It is because of its unique, stable and non-invasive characteristics. Iris recognition is the process of recognizing an individual by analyzing the random pattern of the iris and comparing it with that of reference in the database. The iris is an annular part between the pupil (black portion) and sclera (white portion) of an eye image. It is a muscle within the eye that regulates the size of the pupil. Generalized block diagram of iris recognition system is shown in Fig. 1. The system is divided into enrollment and authentication modules. The enrollment process consists of iris acquisition, segmentation, normalization, enhancement and extraction of features from the iris image. These features are stored into the database (DB) as reference. During the verification process, the matching algorithm is used to compare the test iris features with stored features.

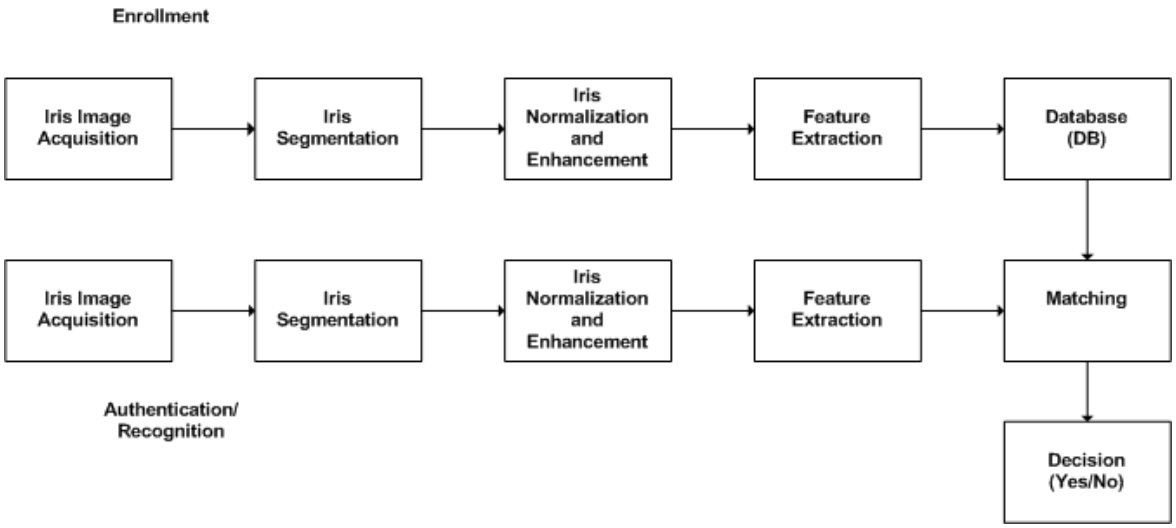

Fig.1. Generalized Block Diagram of Iris Recognition System

The main task of an iris recognition system is the feature extraction. It derives the features with discriminating capability from normalized iris image. The feature extraction can be generally classified into three main categories-phase based method, zero-crossing detection and texture based method. Daughman [1]-[3], Meng and Xu [4], Proenca and Alexandre [5] used multiscale quadrature Gabor wavelet and Masek [6], Vatsa *et al.* [7] used Log-Gabor wavelet to extract phase information of the iris. Boles and Boashash [8], Martin-Roche *et al.* [9], Sanchez–Avila *et al.* [10] used 1-D wavelet transform (WT) to compute the zero-crossing representation at different resolution levels of a concentric circle on an iris image. Wildes [11] proposed the characterization of iris texture through Laplacian pyramid with four different resolution levels. Lim *et al.* [12] used 2-D Haar wavelet transform to decompose an iris image into four levels. Ma *et al.* extracted the texture features of an iris using Gabor [13], a bank of spatial filters [14] and WT [15]. Y. Zhu *et al.* [16] presented multi-channel Gabor filtering and discrete wavelet transform to extract global texture features. S. Helen and Selvan used contourlet transform to extract the iris texture [17]. Nabti *et al.* [18] proposed the feature extraction technique which is based on a combination of special Gabor filter and wavelet maxima components. Altun A. A. [19] used the first generation curvelet transform to denoise (enhanced) the fingerprint and iris images and used 2-D Gabor wavelet for the feature extraction with the use of genetic algorithm (GA).

The main problem with the existing iris recognition techniques is quality of an eye image and precise representation of random iris pattern. The recognition will be accurate when images are free from artifacts and the representation of iris structure is exact. It is observed that iris consists of many irregular small blocks (texture) which are random in nature (crypts, radial streaks, radial furrows, coronas, freckles, collarette, ring, etc). It is very difficult to locate such features, specially elongated or anisotropic features using transforms like Discrete Wavelet Transform (DWT), Dual Tree-Complex Wavelet Transform (DT-CWT) and Gabor. So to localize the aforementioned iris features, we have proposed the use of second generation curvelet transform known as 2-D Fast Discrete Curvelet Transform (FDCT) to derive anisotropic iris feature vector. The images are classified using the nearest neighbor classifier based on Euclidean distance. The technique yields good recognition rate and low error rates. The proposed scheme is scale, translation and rotation invariant. Also, it works effectively in presence of artifacts.

The rest of the paper is organized as follows. Section 2 describes the iris preprocessing. The detail description of the proposed feature extraction scheme is presented in Section 3. Experimental results are reported in Section-4. This is followed by conclusion in Section 5.

2. IRIS PREPROCESSING

An acquired eye image is shown in Fig. 2(a). The first step of iris recognition deals with iris segmentation (iris separation). The iris is segmented by localizing the inner (pupillary) and outer (limbic) boundaries. An integro-differential operator [1]-[3] is used to separate the iris from an eye image which is given by

$$\left| G_\sigma(r) * \frac{\partial}{\partial r} \oint_{x0,y0,r} \frac{I(x,y)}{2\pi r} ds \right| \quad (1)$$

This operator searches over the image domain *(x, y)* for the maximum change in the blurred partial derivative with respective to increasing radius *r* of the normalized contour integral of *I(x, y)* along a circular arc of radius *r* and center coordinate (x_0, y_0). In this, G_σ is a smoothing function such as a Gaussian of scale σ, Δr is a small increment in radius, and $\Delta\theta$ is the angular sampling interval along the circular arcs. The segmented iris is shown in Fig. 2(b).

The segmented iris is normalized to compensate variations in the pupil's size and imaging distances. It involves unwrapping of iris and converting it into fixed size. This is done with the help of Daughman's rubber sheet model [1]-[3] using linear interpolation as below.

$$I(r,\theta) = I[x(r,\theta), y(r,\theta)], \quad (2)$$

where

$$\begin{bmatrix} x(r,\theta) \\ y(r,\theta) \end{bmatrix} = \begin{bmatrix} xp(\theta) & xl(\theta) \\ yp(\theta) & yl(\theta) \end{bmatrix} \begin{bmatrix} 1-r \\ r \end{bmatrix} \quad (3)$$

$(xp(\theta), yp(\theta))$ and $(xp(\theta), yp(\theta))$ are the pupillary boundary and limbic boundary coordinates respectively, $r \in [0,1]$ and $\theta \in [0,2\pi]$. The normalized iris image is shown in Fig.2(c). The normalization is also used to achieve the scale and translation invariance.

The normalized image has still low contrast and non-uniform brightness which is caused by the position of light sources. In order to obtain well distributed texture image (enhanced iris image), we have used the background subtraction method proposed by L. Ma *et al*. [14], [15]. The steps for iris image enhancement are given below.

1. First, the mean of each 16x16 small blocks are computed to constitute a coarse estimate of the background illumination.
2. This estimate is further expanded to the same size as the normalized image by bicubic interpolation.
3. This estimated background illumination image is subtracted from the normalized image to compensate for a variety of lighting conditions.
4. Then, enhanced the lighting corrected image by means of histogram equalization in each 32x32 region to compensate for non-uniform illumination and improve the contrast of an image. The enhanced iris image is shown in Fig. 2(d).

In order to extract the local features, enhanced iris image is divided into six sub-regions. The vertically partitioned iris image is shown in Fig. 2(e) (four sub-images) whereas Fig. 2(f) shows the horizontally partitioned iris image (two sub-images).

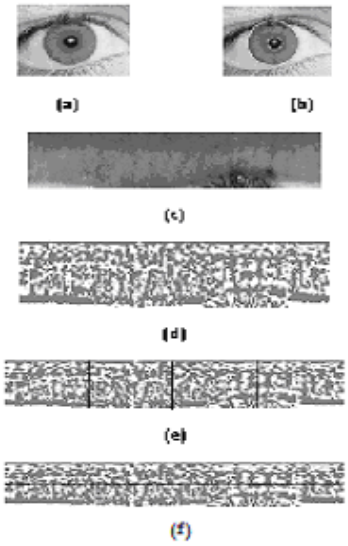

Fig.2(a) Original eye image. (b) Segmented iris image. (c) Normalized Image. (d) Enhanced Image. (e) Vertically partitioned iris image. (f) Horizontally partitioned iris image

3. FEATURE EXTRACTION

It is observed that enhanced normalized iris image consists of mostly curvilinear features. In this paper, 2-D FDCT via wrapping is used to extract the significant anisotropic iris features (curvelet coefficients). The feature vector is created by estimating the energies of these curvelet coefficients.

3.1. CURVELET TRANSFORM

The curvelet transform is proposed for image denoising by Starck *et al.* [20] and has shown promising performance over DWT. Since curvelet transform captures curvilinear information perfectly, it has shown promising results in content based image retrieval [21], character recognition [22], face recognition [23] etc. The curvelet transform has been divided into two generations. The first generation curvelet transform (commonly called as "curv99") is proposed by Candes and Donoho [24]. It involved ridgelet analysis and hence is extremely slow. Therefore, the algorithm was modified where the ridgelet analysis has been removed (redundancy reduction) to increase the speed. The curvelet has a frequency support in a parabolic-wedge area due to the anisotropic scaling law as *width* = *length*^{2} as shown in Fig. 3. The two algorithms based on this theoretical basis are known as Discrete Curvelet Transform [25].

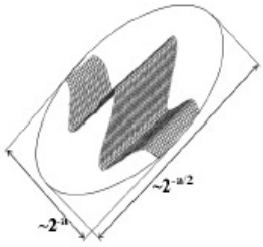

Fig.3. Single Curvelet

The first algorithm is Fast Discrete Curvelet Transform (FDCT) via unequally-spaced Fast Fourier Transform (USFFT). In this algorithm, curvelet coefficients are obtained by irregularly sampling the Fourier coefficients of an image. The second algorithm known as FDCT via wedge-wrapping is based on the series of translation and wrapping of specially selected Fourier samples. Both the algorithms are used to give the same output but FDCT via wrapping is more intuitive and faster [25].

The curvelet transform is a multiscale geometrical transform with frame elements given by scale, location and orientation parameters. It has not only the time-frequency localization properties of wavelet but also shows a very high degree of directionality. It is also observed that curvelet transform covers whole frequency spectrum so that there is no loss of information. Fig. 4 shows the curvelet tiling and cover of spectrum with 5 scales on dyadic concentric square coronae [25]. The shaded trapezoid (i.e. wedge-area) shows the frequency response of curvelet at orientation 4 and scale 4.

The 2-D discrete curvelet transform is expressed as

$$C^D(j,l,k) = \sum_{0\le m<M, 0\le n<N} f[m,n] \cdot \varphi^D_{j,l,k}[m,n] \quad (4)$$

where $f[m,n], 0 \le m < M, 0 \le n < N$ is the input 2-D image. $C^D(j,l,k)$ are the discrete curvelet coefficients, $\varphi^D_{j,l,k}$ is the curvelet basis function, j is the scale, $l \in R$ is the location and $k \in [0,2\pi]$ is the orientation. In this paper, 2-D FDCT via wrapping is used as it is simpler, less redundant and faster.

The architecture of FDCT via wrapping is as follows [25]

1. The 2-D FFT is applied on the image to obtain Fourier samples $\tilde{f}$.
2. The product $\tilde{U}_{j,l} \cdot \tilde{f}$ is obtained for each scale j and angle l, where $\tilde{U}_{j,l}$ is the parabolic window (curvelet window) which is basically computed in the frequency domain.
3. The aforementioned product wraps around the origin and obtain
   $$\tilde{f}_{j,l}[n_1,n_2] = W\left(\tilde{U}_{j,l}\tilde{f}\right)[n_1,n_2] \quad (5)$$
   where the range for n_1 and n_2 *is* $0 \le n_1 < L_{1,j}$ and $0 \le n_2 < L_{2,j}$. $L_{1,j}$ and $L_{2,j}$ are the dimensions of the rectangle. The wrapping approach is shown in Fig. 5.
4. The discrete curvelet coefficients $C^D(j,l,k)$ are obtained with the help of inverse 2-D FFT to each $\tilde{f}_{j,l}$. In this work, Fig. 3 which shows the single curvelet, Fig. 4 that shows tiling of curvelet construction and Fig.5 showing wrapping mechanism have been produced from Candes *et al.* [25] (with permission).

3.2 FEATURE VECTOR

The normalized directional energy is computed from each sub-band of the curvelet to form the feature vector. To compute the energies using L_1 norm, the following expression is used.

$$E_k = \frac{1}{M \times N} \sum_{i=1}^{M} \sum_{j=1}^{N} \left| x_k(i, j) \right| \quad (6)$$

where E_k is the energy of the k^{th} sub-band of curvelet and $x_k(i,j)$ is the corresponding sub-band with dimension $M \times N$.

Hence, for each scale and direction, anisotropic features are derived and the resultant feature vector is as given by (7).

$$f = [f_{E1}, f_{E2}, f_{E3}, \ldots] \quad (7)$$

3.3 RECOGNITION RULE

The feature vectors are derived from each of the normalized iris images during enrollment process. The test iris feature vector is compared with stored vectors using Euclidean distance (ED) given as

$$ED_i = \left(\sum_{i=1}^{N} \left(T_i - E_i \right)^2 \right)^{\frac{1}{2}} \quad (8)$$

where N is the dimension of feature vector. T_i is the i^{th} component of test feature vector and E_i is i^{th} component of enrolled feature vector. The test image is verified on the basis of minimum distance (Nearest Neighbor classifier).

Following steps describe the algorithm in detail: -

1. Iris image is segmented using integro-differential operator.
2. The segmented iris image is normalized using Daughman's rubber sheet model.
3. The background subtraction method is used to enhance normalized iris image.
4. This enhanced normalized image is divided into six sub-regions.
5. The 2-D FDCT via wrapping is used separately on each of these six sub-regions to extract local features (also called as curvelet coefficients).
6. Six local feature vectors are derived by estimating energies of curvelet coefficients of each sub-region.
7. These six local feature vectors are combined to create the resultant local feature vector (template).

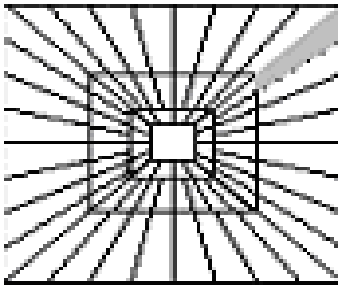

Fig.4. Curvelet Tiling of Frequency Plane. The Shaded Area represents Generic Wedge

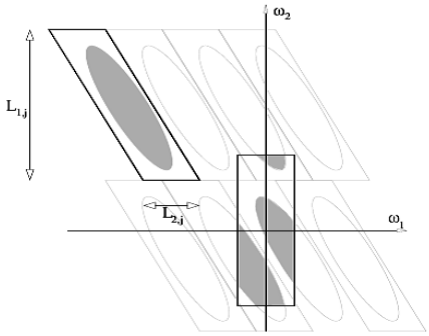

Fig.5. Wrapping Data, Initially inside a Parallelogram into a Rectangle by Periodicity

4. EXPERIMENTAL RESULTS

In this paper, performance of the proposed approach is evaluated using two databases: (1) UBIRIS and (2) MMU1. The effectiveness of this method is shown in terms of absolute performance index and comparative performance against some existing popular feature extraction schemes such as Gabor[13], DWT[16], and DT-CWT[28]. Following sets of experiments were carried out

1. Computation of recognition rate
2. Computation of FAR/FRR.
3. Computational complexity.

4.1 DATABASE

The performance of the proposed approach is tested on the two databases namely UBIRIS[26] and MMU1[27]. The images are captured from different instruments under varying conditions and from different ethnicity. The UBIRIS database consists of 1877 iris images of 241 persons captured in two different sessions using Nikon E5700 camera. The images in this database include the artifacts in the form of reflection, contrast, natural luminosity, focus and eyelids/eyelashes obstructions. The MMU1 database consists of 45 persons having 5 images of left and 5 images of right eye. Thus it includes total 450 images of 90 subjects. These images are captured with LG IrisAccess camera which contains, exclusively, iris obstructions by eyelids/eyelashes and specular reflection. We have selected 450 images of 90 subjects (with 5 images per subject) randomly from UBIRIS database (including session1 and session2) which are captured under non-ideal environmental conditions whereas all the images from MMU1 database have been used for the experimentation.

4.2 PREPROCESSING AND FEATURE EXTRACTION

Iris is separated by locating the inner and outer boundaries of the iris with the assumption that both boundaries are circular in nature. The scale and translation invariance is achieved using normalization technique as given in Section 2. In order to achieve the rotation invariance, the iris ring is converted into rectangular fixed block of size 64×360 with five initial angles -10^0, -5^0, 0^0, 5^0, 10^0. For enrollment, two iris images per subject

have been used. In this process, five normalized images corresponding to angles -10^0, -5^0, 0^0, 5^0, 10^0 are obtained. Thus the total number of enrolled images for each person is 10. The 2-D FDCT is applied on the normalized iris image to extract the anisotropic features.

4.3 COMPUTATION OF RECOGNITION RATE

In this set of experiment, two images per subject (with five angles) from each database have been used for training and five images per subject have been used for testing. ED between test feature vector and training feature vectors are computed. The test image is classified on the basis of minimum distance using the nearest neighbor classifier. The recognition rate (RR) is computed as below.

$$RR=\frac{\text{No.of correct matches}}{\text{Total no. of test images}}\times 100\% \quad (9)$$

In the first part of the experiment, features of iris are extracted globally (by using complete normalized enhanced iris) using the proposed algorithm. In the subsequent part, local features are computed by dividing the normalized enhanced iris image into six sub-images. The performance of proposed approach is compared with the existing techniques (DWT(db3), DT-CWT, and Gabor) for both local and global feature extraction techniques. The recognition rates of these techniques are compared in Table 1 and Table 2 for global and local feature extraction approaches respectively.

Table.1 RR for Different Feature Extraction Algorithms using Global Features

Algorithms	%RR	
	UBIRIS Database	MMU1 Database
DWT	91.33	84.89
DT-CWT	90.67	79.33
Gabor	90.22	81.56
2-D FDCT	**92.22**	**83.33**

Table.2 RR for Different Feature Extraction Algorithms using Local Features

Algorithms	%RR	
	UBIRIS Database	MMU1 Database
DWT	95.56	92.67
DT-CWT	95.56	82.44
Gabor	96.00	89.78
2-D FDCT	**96.44**	**92.89**

It is observed that local (partitioned) approach significantly improves the performance.

DWT gives information in only three directions i.e. horizontal, vertical, and diagonal. The extension of DWT is DT-CWT which also gives limited directional information (six directions). Both DWT and DT-CWT are best suited for point singularities but not good for curvilinear singularities. Although Gabor transform derives more angular information, there is information loss in its spectral domain. Also, Gabor transform introduces redundancy. The better performance of proposed approach is because of the extraction of anisotropic and more directional features of iris image.

4.4 COMPUTATION OF FALSE ACCEPTANCE RATE (FAR) FALSE REJECTION RATE (FRR)

The performance of proposed algorithm has been evaluated using Receiver Operating Characteristics (ROC). It consists of performance measure of False Acceptance Rate (FAR) and False Rejection Rate (FRR) at different values of thresholds. The correct recognition rate, is obtained when two feature vectors of the same individual are compared and an imposter matching score is obtained when feature vectors of different individuals are compared. FAR is the probability of accepting an imposter as a genuine subject and FRR is the probability of a rejecting a genuine subject.

For an individual, images excluding his own images will be the imposters. FRR is computed using following expression.

FRR = (True claims rejected/Total true claims) x 100% (10)

FAR is computed by counting the number of imposter's claims accepted out of total imposter's claims for given threshold.

FAR = (Imposter claim accepted/Total imposter claims) x 100% (11)

Table.3. Error rates for Different Feature Extraction Algorithms using Global Features

Algorithms	%Error Rates			
	UBIRIS Database		MMU1 Database	
	FAR (%)	FRR (%)	FAR (%)	FRR (%)
Gabor	9.57	9.78	18.05	18.44
DWT	8.45	8.67	15.09	15.11
DT-CWT	9.25	9.33	19.74	20.67
2-D FDCT	**7.34**	**7.78**	**15.94**	**16.67**

Table.4. Error rates for Different Feature Extraction Algorithms using Local Features

Algorithms	%Error Rates			
	UBIRIS Database		MMU1 Database	
	FAR (%)	FRR (%)	FAR (%)	FRR (%)
Gabor	4.05	4.00	10.00	10.22
DWT	4.36	4.44	7.29	7.33
DT-CWT	4.41	4.44	17.40	17.56
2-D FDCT	**3.51**	**3.56**	**6.82**	**7.11**

In verification mode, test iris feature vector is compared with enrolled feature vectors of 10 images from a person and used minimum distance (compared with the threshold) to authenticate the person. Thus, inter and intra class EDs are obtained to estimate FAR and FRR. To evaluate the performance of proposed approach, we have used local and global iris feature vectors. The performance of the proposed approach is compared with existing techniques (DWT (db3), DT-CWT, Gabor

transform). In our experimentations, total numbers of inter and intra class comparisons for each database are 200250 and 4500 respectively.

Table.3 shows FAR and FRR of global feature extraction approach. Fig. 6 and Fig.7 show ROC curves with different values of thresholds on UBIRIS and MMU1 databases respectively. The similar results for local feature extraction approach are given in Table 4, Fig. 8 and Fig. 9.

The results show that the proposed feature extraction scheme is superior as compared to existing techniques (low error rates).

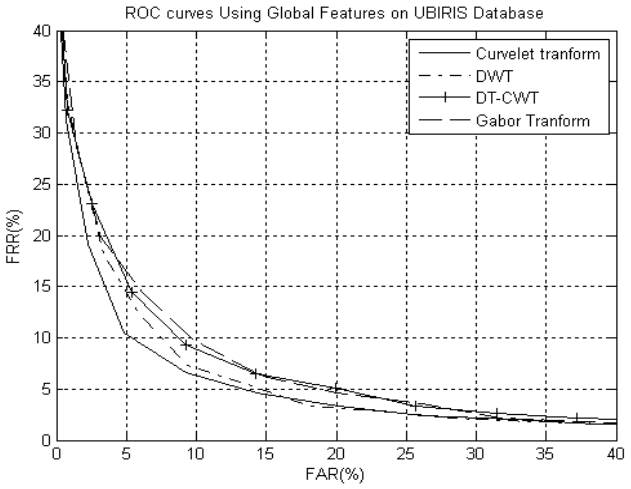

Fig.6. ROC Curves for Different feature extraction Algorithms on UBIRIS database using Global Features

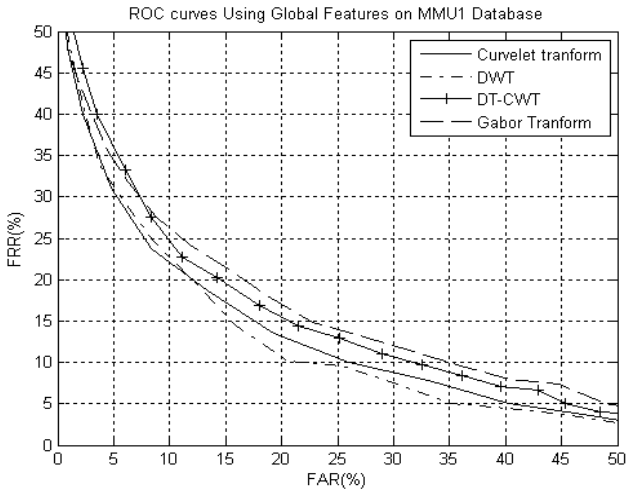

Fig.7. ROC Curves for Different Feature Extraction Algorithms on MMU1 Database Using Global Features

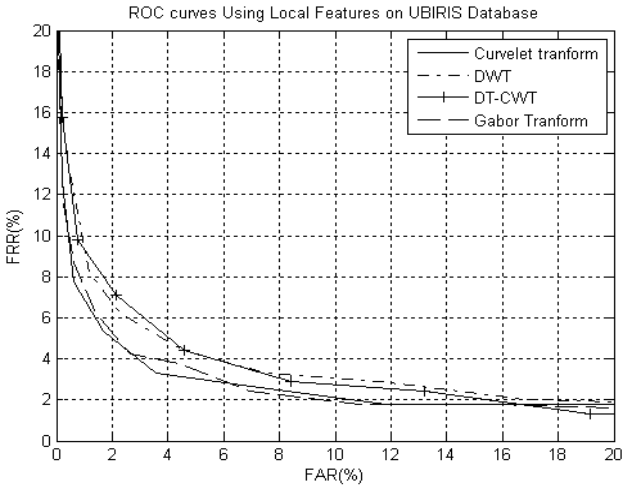

Fig.8. ROC for Different Feature Extraction Algorithms on UBIRIS database using Local Features

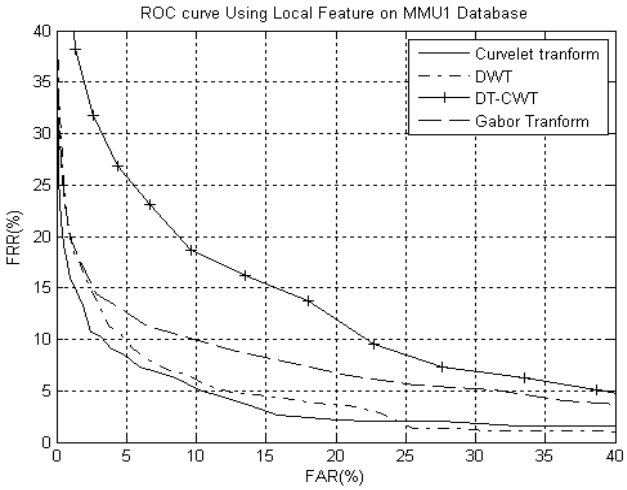

Fig.9. ROC for Different Feature Extraction Techniques on MMU1 Database Using Local Features

5. CONCLUSION

In this paper, we have proposed the feature extraction method for iris recognition using FDCT. It extracts anisotropic local features and provides more directional information. The anisotropic feature vector is derived from the six sub-images of normalized enhanced iris image using FDCT. The proposed method gives FAR of 3.51% and FRR of 3.56% in case of UBIRIS database and FAR of 6.82% and FRR of 7.11% on MMU1 database which is better than some of the existing techniques (DWT, DT-CWT, and Gabor). The proposed approach is scale, translation and rotation invariant. The experimental results show boost in performance of the proposed scheme under non-ideal environmental conditions (without removal of eyelids/eyelashes occlusion and specular reflection etc.).

ACKNOWLEDGEMENT

The authors are very much thankful to the editor and anonymous reviewers for their constructive comments and valuable suggestions. The authors also would like to thank Dr. Nick Kingsbury and curvelet team for providing us the material on curvelet transform and DT-CWT respectively.

REFERENCES

[1] Daughman, J. G, 1993, "High confidence of visual recognition of persons by a test of statistical independence". *IEEE Trans. on Pattern Analysis and Machine Intelligence,* Vol. 15, No. 11, pp.1148-1161.

[2] Daughman, J. G, 2003, "The importance of being random: statistical principles of iris recognition". *Pattern Recognition*, Vol.36, No. 2, pp. 279-291.

[3] Daughman, J. G, 2004, "How iris recognition works". *IEEE Trans. On Circuits and System for Video Technology,* Vol.14, No.1, pp. 21-30.

[4] Meng, H. and Xu, C, 2006, "Iris recognition algorithm based on Gabor wavelet transform" in *Proc. of the IEEE, International Conference on Mechatronics and Automation.*

[5] Proenca, H. and Alexandre, L. A, 2007, "Toward noncoperative iris recognition: A classification approach using multiple signatures". *IEEE Trans. On Pattern Analysis and Machine Intelligence,* Special Issue on Biometrics, Vol. 9, No. 4, pp. 607-612.

[6] Masek, L, 2003, "Recognition of human iris pattern for biometric identification". M. Thesis, University of Western Australia.

[7] Vatsa, M., Singh, R. and Noore, A, 2008, "Improving iris recognition performance using segmentation, quality enhancement, match score fusion, and indexing". *IEEE Trans. On Systems, Man, and Cybernetics-Part B: CYBENETICS,* Vol. 38, No.4, pp. 1021-1034.

[8] Boles, W. W. and Boashash, B, 1998, "A Human identification technique using images of the iris and wavelet transform". *IEEE Trans. On Signal Processing,* Vol. 46, No. 4, pp. 1185-1188.

[9] de Martin-Roche, D., Sanchez-Avila, C. and Sanchez-Reillo, R, 2001, "Iris recognition for biometric identification using dyadic wavelet transform zero crossing", in Proc. *International Carnahan Conference* on Security Technology (London, England), pp. 229- 234.

[10] Sanchez-Avila, C., Sanchez-Reillo, R. and de Martin-Roche, D, 2002, "Iris based biometric recognition using dyadic wavelet transform". *IEEE Aerospace and Electronic Systems Magazine*, Vol. 17, No. 10, pp. 3-6.

[11] Wildes, R.P., 1997, "Iris Recognition: An emerging biometric technology", in *Proc. of the IEEE*. Vol. 85, No. 9, pp. 1348-1363.

[12] Lim, S., Lee, K., Byeon, O. and Kim, T, 2001, "Efficient iris recognition through improvement of feature vector and classifier". *ETRI journa,*. Vol. 23, No. 2, pp. 61-70.

[13] Ma, L., Wang, Y. and Tan, T, 2002, "Iris recognition based on multichannel Gabor filtering", in *Proc. Of the 5th Asian Conference on Computer Vision,* pp. 279-283

[14] Ma, L, Tan, T., Wang Y. and Zhang D, 2003, "Personal identification based on iris texture analysis". *IEEE Trans. on Pattern Analysis and Machine Intelligence*, Vol.25, No.12, pp. 1519-1533.

[15] Ma, L., Tan, T., Wang, Y. and Zhang D, 2004, "Efficient iris recognition by characterizing key local variation". *IEEE Trans. on Image processing*, Vol. 13, No. 6, pp. 739-750.

[16] Zhu, Y., Tan, T. and Wang,Y, 2000, "Biometric Personal Identification Based on Iris Pattern", in *Proc. ICPR' 2000,* Vol. 2, pp. 801-804.

[17] Helen, S. C. and Selvan, S, 2006, "Iris feature extraction based on Directional Image Representation. *GVIP Journal,* Vol. 8, No. 4, pp. 55-62.

[18] Nabti, M., Ghouti, L. and Bouridane, A, 2008, "An effective and fast iris recognition system based on a combined multiscale feature extraction technique". *Pattern Recognition,* Vol. 41, pp. 868-879.

[19] Altun, A. A, 2008, "Recognition of selected fingerprint and iris features enhanced by curvelet transform with Artificial Neural network", in *Proc. IWSSIP' 2008*, pp. 421-424.

[20] Starck, J., Candes, E.J., and Donoho, D. I, 2002, "The Curvelet Transform for Image Denoising". *IEEE Trans. On Image Processing,* Vol. 11, No. 6, pp. 670-684.

[21] Sumana, I. J., Islam M. M., Zhang, D. and Lu, G, 2008, "Content Based Image Retrieval Using Curvelet Transform", in *Proc. of IEEE International workshop on multimedia signal processing*, MMSP08, pp. 11-16.

[22] Majumdar, A, 2006, "Bangla Basic Character Recognition using Digital Curvelet Transform". *Journal of Pattern Recognition Research,* Vol.2, No. 1, pp. 17-26.

[23] Zhang, J., Zhang, Z., Huang, W., Lu, Y. and Wang, Y. 2007, "Face Recognition Based on Curvefaces", in *Proc. ICNC' 2007,* Vol. 2, pp. 627-631.

[24] Candes, E. J. and Donoho, D. I, 2000, "Curvelets-a surprisingly effective nonadaptive representation for objects with edge". *Saint-Malo 1999*, A. Cohen, C. Rabut, L. Schumaker (Eds.), Vanderbilt Univ. Press, Nashville, pp.105-120.

[25] Candes, E. J., Demanet, L., Donoho, D. L. and Ying, L, 2005, "Fast Discrete Curvelet Transform. Technical Report", CalTech.

[26] Proenca, H. and Alexandre, L. A. UBIRIS: A noisy iris image database, webste: http://www.iris.di.ubi.pt.

[27] Multimedia university iris database, http://www.pesona.mmu.edu.my/~ccteo/.

[28] Selesnick, I. W., Baraniuk, R. G. and Kingsbury, N.G, 2005, "The Dual Tree Complex Wavelet Transform". *IEEE Signal Processing Magazine,* Vol. 22, No. 6, pp. 123–151.